molecules

MDPI

Article

Streptomyces rochei MS-37 as a Novel Marine Actinobacterium for Green Biosynthesis of Silver Nanoparticles and Their Biomedical Applications

Sobhy E. Elsilk [1], Maha A. Khalil [2,*], Tamer A. Aboshady [3], Fatin A. Alsalmi [2] and Sameh S. Ali [1,4,*]

[1] Botany and Microbiology Department, Faculty of Science, Tanta University, Tanta 31527, Egypt
[2] Biology Department, College of Science, Taif University, P.O. Box 11099, Taif 21944, Saudi Arabia
[3] Oral and Maxillofacial Surgery and Diagnostic Sciences, Faculty of Dentistry, Taif University, Taif 21944, Saudi Arabia
[4] Biofuels Institute, School of the Environment and Safety Engineering, Jiangsu University, Zhenjiang 212013, China
* Correspondence: maha.ak@tu.edu.sa (M.A.K.); samh@ujs.edu.cn (S.S.A.)

Abstract: Periodontitis, as one of the most common diseases on a global scale, is a public health concern. Microbial resistance to currently available antimicrobial agents is becoming a growing issue in periodontal treatment. As a result, it is critical to develop effective and environmentally friendly biomedical approaches to overcome such challenges. The investigation of *Streptomyces rochei* MS-37's performance may be the first of its kind as a novel marine actinobacterium for the green biosynthesis of silver nanoparticles (SNPs) and potentials as antibacterial, anti-inflammatory, antibiofilm, and antioxidant candidates suppressing membrane-associated dental infections. *Streptomyces rochei* MS-37, a new marine actinobacterial strain, was used in this study for the biosynthesis of silver nanoparticles for various biomedical applications. Surface plasmon resonance spectroscopy showed a peak at 429 nm for the SNPs. The SNPs were spherical, tiny (average 23.2 nm by TEM, 59.4 nm by DLS), very stable (−26 mV), and contained capping agents. The minimum inhibitory concentrations of the SNPs that showed potential antibacterial action ranged from 8 to 128 µg/mL. Periodontal pathogens were used to perform qualitative evaluations of microbial adhesion and bacterial penetration through guided tissue regeneration membranes. The findings suggested that the presence of the SNPs could aid in the suppression of membrane-associated infection. Furthermore, when the anti-inflammatory action of the SNPs was tested using nitric oxide radical scavenging capacity and protein denaturation inhibition, it was discovered that the SNPs were extremely efficient at scavenging nitric oxide free radicals and had a strong anti-denaturation impact. The SNPs were found to be more cytotoxic to CAL27 than to human peripheral blood mononuclear cells (PBMCs), with IC_{50} values of 81.16 µg/mL in PBMCs and 34.03 µg/mL in CAL27. This study's findings open a new avenue for using marine actinobacteria for silver nanoparticle biosynthesis, which holds great promise for a variety of biomedical applications, in particular periodontal treatment.

Keywords: marine actinobacteria; silver nanoparticles; antibacterial; anti-inflammatory; antibiofilm; cytotoxicity

Citation: Elsilk, S.E.; Khalil, M.A.; Aboshady, T.A.; Alsalmi, F.A.; Ali, S.S. *Streptomyces rochei* MS-37 as a Novel Marine Actinobacterium for Green Biosynthesis of Silver Nanoparticles and Their Biomedical Applications. *Molecules* **2022**, *27*, 7296. https://doi.org/10.3390/molecules27217296

Academic Editor: Chiara Brullo

Received: 13 September 2022
Accepted: 25 September 2022
Published: 27 October 2022

1. Introduction

Periodontitis is an inflammatory disease that affects the teeth's supporting structures, resulting in the gradual deterioration of periodontal tissues, loss of attachment, aesthetics, and, eventually, tooth loss [1]. Even though there are numerous causes of periodontitis, bacterial plaque is frequently identified as the primary etiological agent of this oral disease [2]. Dental plaque is a biofilm formed by bacteria on the surface of teeth, gingiva, and restorative or prosthetic materials [3]. *Staphylococcus* spp., *Streptococcus mutans*, *Porphyromonas gingivalis*, and *Aggregatibacter actinomycete mcomitans* are among the bacteria implicated in the etiology of periodontitis, with *Staphylococcus* being the most common

bacterium responsible for microbial infections associated with biofilms [4]. Periodontal treatment's major objective is to destroy the microbial biofilm and decrease inflammation to establish and maintain sufficient infection control [5]. Numerous antimicrobial medicines have been utilized to treat periodontal disease. Mechanical removal of plaque and frequent application of systemic and topical antibacterial medications are only partially successful against the microorganisms responsible for periodontal diseases [6]. As a result, various agents with advanced physicochemical characteristics should be investigated, emphasizing antibacterial agents with innovative and distinct features that may be utilized as a substitute for periodontal treatments. Periodontal regeneration requires the isolation of gingival epithelial and connective tissue cells from the injured area, which results in the invention and implementation of guided tissue regeneration (GTR) membranes [7]. The regeneration of various intrabody lesions has been accomplished with effectiveness and dependability using GTR procedures using non-absorbable and bioabsorbable membranes. Rossa et al. [8] emphasized the importance of containing or eliminating periodontal infections for barrier membranes to reattach. Several techniques for managing or eradicating periodontal infections during GTR treatments have been promoted [9,10].

Inflammation is a physiological response to potentially harmful stimuli such as irritants, damaged tissue, or infections [11]. Systemic or localized inflammation can be acute or chronic [12]. Numerous mediators, such as prostaglandins, cytokines, and various reactive oxygen species (ROSs), such as nitric oxide (NO), are produced by various immune cell types or neutrophil respiratory bursts to protect cells and tissues during the acute inflammatory phase [13]. Synthetic medicines, formerly extensively used to treat inflammation, are no longer safe due to drug-related toxicity, iatrogenic responses, and dangerous adverse reactions that hinder therapy progression when administered long-term [14]. A safer and more effective alternative to conventional medicine, which has demonstrated efficacy in treating a variety of human disorders over the past several decades, must be developed as a result.

Recently, nanomaterials as treatments have emerged as a novel strategy for preventing and controlling the spread of many serious diseases [15–19]. Silver nanoparticles (SNPs) have displayed remarkable biocidal properties against a variety of pathogens, including some oral bacteria [20–23], and have even demonstrated superior antimicrobial properties to dental antiseptic solutions, which are considered essential in a dental clinic [24]. SNPs possess unique optical, electromagnetic, catalytic, and electrical characteristics, resulting in their extensive application as antimicrobial, anti-inflammatory, and anticancer medicines [25–27]. SNPs have been synthesized using a variety of methods, including classical (physical and chemical) and biological procedures [28–30]. Researchers have employed extreme reaction tracking to determine the difference between the biochemical reduction of nanoparticles using green production and a conventional approach [31–34]. Green nanoparticles had considerably lower cytotoxicity than chemical nanoparticles, suggesting that they are safe and may be used widely in biomedical applications [17,18,35]. For the manufacture of nanoparticles, green synthesis techniques such as bacteria, in particular actinobacteria, fungi, yeast, and plants, may be employed [36,37]. Amongst them, actinobacteria are a frequent source of SNPs with anticancer, antioxidant, and antimicrobial properties [21].

Several studies have recently focused on silver nanoparticles, and few studies have been published on actinobacteria, in particular *Streptomyces rochei*, with the ability to produce nanoparticles [38]. However, the effectiveness of SNPs in periodontal therapy, notably marine actinobacteria, remains unexplored or at its early stage. To the authors' knowledge, no studies have been undertaken so far to investigate the performance of *Streptomyces rochei* MS-37 as a new marine actinobacterium for green biosynthesis of SNPs valued for antibacterial action against gingival pathogens and their effectiveness in periodontal treatment. Therefore, the current research focuses on the production of silver nanoparticles using *Streptomyces rochei* MS-37 and the elucidation of their antibacterial efficacy against oral pathogenic bacterial strains. In addition, the effectiveness of bio-SNPs' antibiofilm and anti-

inflammatory potential and antioxidant possibilities in decreasing membrane-associated dental infections was evaluated.

2. Materials and Methods

2.1. Cell Culture

Cell culture flasks (75 cm^3, 250 mL volume) with 10% fetal bovine serum (FBS; Life Technologies, Gibco®; Carlsbad, CA, USA) and 50 g/mL gentamicin were used to cultivate the CAL27 oral adenosquamous carcinoma cells. Cells were cultured in Dulbecco's modified Eagle's medium (DMEM; Life Technologies, Gibco®; Carlsbad, CA, USA) (Naviform, Annapolis, GO, Brazil). Daily, cultures were examined under an inverted microscope while being incubated in 37 °C incubators with 5% CO_2. When cell growth achieved a confluence of 70–80% of the total volume of the culture flask, cells were detached using trypsin. Centrifugation was used to separate human peripheral blood mononuclear cells (PBMCs) using a Ficoll density gradient (Ficoll-Paque Plus; GE Healthcare Bio-Sciences AB; Chicago, IL, USA). After two washes with saline, cells (0.3×10^6 cells/mL) were resuspended in RPMI media supplemented with 20% FBS, 2 mM glutamine, and 50 µg/mL gentamicin.

2.2. Nanoparticle Biosynthesis

Actinobacterial strain MS-37 was cultivated for 7 days at 28 °C on a starch casein agar medium [39]. MS-37 was molecularly characterized using 16S rDNA gene sequencing, as published by Khalil et al. [22]. The actinobacterial biomass was centrifuged at 6000× *g* for 10 min, cleaned three times in sterile distilled water, and then autolyzed for three days at 28 °C in the same sterile distilled water. The cell debris was removed by centrifugation at 6000 rpm for 15 min, and the secondary metabolites of the actinobacterium were combined with silver nitrate ($AgNO_3$; 1 mM final concentration; Sigma Aldrich) as a precursor to create SNPs. A 20 µL aliquot of overnight-grown *Streptomyces rochei* MS-37 was inoculated into 100 mL of nutrient broth medium, which was subsequently incubated on an orbital shaker at 28 °C and 120 rpm for 96 h [40]. After incubation, the actinobacterium biomass was collected by 30 min of centrifugation at 5000 rpm. To remove associated media components, 2 g of cells was washed twice with distilled water. The biomass was reconstituted in 150 mL of deionized water and stored at 28 °C for 48 h. Bacteria were lysed osmotically, then filtered via Whatman No. 1 filter paper. As previously reported by [21,41], the concentration of the stock colloidal solution of the synthesized SNPs (1.7 µL/mg) was determined using the formulae presented by Liu et al. [42].

2.3. Characterization of SNPs

Both visually and spectroscopically, UV spectroscopy (Nano Drop ND2000, Thermo Scientific, Waltham, MA, USA) in the wavelength range of 300–800 nm with a resolution of 1 nm was used to observe the synthesis of the SNPs. The control sample was the autolyse without silver nitrate. To extract the biosynthesized SNPs, 13,000× *g* centrifugation for 1 h was utilized. For mass determination, the resulting nanoparticles were purified by washing with double-distilled water, organic solvents (ethanol), and drying at 40 °C. The size and shape of the SNPs were determined using TEM (JEM-1230, JEOL, Tokyo, Japan), which operated at a 120 kV acceleration voltage. After application, the SNPs were re-suspended in a carbon-coated copper grid with a 400 m mesh size, molecular grade sterile water, and allowed to dry at ambient temperature. Fourier transform infrared spectroscopy (FTIR; PerkinElmer) was used to depict surface composition variations in more detail [22,43]. The SNPs were pelletized using potassium bromide (KBr) at 1% (*w*/*w*) concentration. The SNPs were crushed for one minute at a pressure of ten tons, followed by FTIR analysis, to produce a clear pellet. Using dynamic light scattering (DLS), the average size and surface charge of the SNPs were determined [44]. Prior to analysis, the SNP sample (1 mg/mL) was diluted 100-fold with MiliQ water and ultrasonically treated to guarantee nanoparticle uniformity. The material was then examined using a Malvern DLS instrument (Nano-Zeta Sizer-HT, Malvern, UK).

2.4. Antibacterial Assays

2.4.1. Isolation and Identification of Oral Pathogenic Bacterial Strains

Clinical pathogenic bacteria were isolated from several gingival sulcus specimens kindly taken from the oral cavity from dental clinics in Taif City, Saudi Arabia. The isolates were sub-cultured on mannitol salt agar and nutrient agar plates. Colonies with a clearly distinct morphology were picked and streaked over the same medium and cultured at 37 °C for 24–48 h. This procedure continued until single pure cultures were obtained. Colony and cell morphology, catalase production, oxidase activity, motility, and Gram reaction confirmed the isolates to the genus level. To characterize the 16S rDNA gene, a partial sequence amplified using genomic DNA as a template and the bacterial universal primers 27F (5′-GAGTTGATCACTGGCTCAG-3′) and 1492R (5′-TACGGCTACCTTGTTACGACTT-3′) were employed. To sequence the purified PCR products, Microgen Co, Seoul, Korea, used the 518F and 800R sequencing primers. Using the NCBI/BLAST tool, the obtained sequences were compared to the reference bacterial species in the gene-bank database. The nucleotide sequence data were deposited, and the accession numbers were obtained from the EMBL nucleotide sequence database.

2.4.2. Susceptibility Testing

Susceptibility to 13 antibiotics was assessed using the standard Kirby–Bauer disc diffusion technique, as approved by the Clinical and Laboratory Standard Institute [45]. The SNPs from strain MS-37 were tested for biological activity against selected gingival pathogens using clinical and Laboratory Standards Institute-recommended fold broth microdilution procedure (CLSI) guidelines [45]. Bacteria were grown in Tryptic Soy Broth (TSB; Becton Dickinson, USA) for 24 h at 37 °C while being shaken at 125 rpm prior to the experiment. The assays were run in triplicate in 96-well plates. The range of the SNPs under investigation was 0.25 to 256 µg/mL, and the final bacterial concentration in each well of a plate was 5 $\times 10^5$ colony forming units (CFU) per ml. Both positive (inoculated medium) and negative (uninoculated media) controls were maintained. Multi-well plates with inoculation were incubated for 24 h at 37 °C. The lowest SNP concentration that prevented bacterial growth was identified visually as the minimum inhibitory concentration (MIC) values. By placing 100 µL of each test sample onto Tryptic Soy Agar (TSA; Becton Dickinson, USA) plates and incubating at 37 °C for 24 h, the minimal biocidal concentration (MBC) values of the SNPs were ascertained. The MBC was found to include the fewest SNPs that could stop >99.9% of bacterial cell development.

2.5. Antibiofilm Activity

The biofilm development experiment in microtiter plates was performed using the procedures described by [46]. TSB (100 µL) was loaded into 96-well flat-bottomed MTPs (Greiner Bio One, Fricken hausen, Mannheim, Germany) with/without supplements. Each well was supplemented with a diluted overnight bacterial culture (1:100 in TSB, 100 µL TSB). The positive control wells contained TSB injected with *S. aureus* ATCC29213, while the negative control wells contained just TSB. Plates were incubated at 37 °C for 18 h before being washed multiple times with PBS (pH 7.3). Sodium acetate (2%) was added as a fixative and decanted, and crystal violet (0.1 percent w/v) was used to stain the wells. Finally, the plates were washed under running tap water, dried, and read with a Sunrise absorbance reader at 570 nm (Tecan Austria GmbH, Salzburg, Austria). Antibiofilm activity was determined following the classification reported by Stepanovic et al [47].

2.6. Nitric Oxide Radical Scavenging Activity

The Griess reaction, which was based on [48], was used to assess the ability of the SNPs to scavenge nitric oxide radicals. The Griess reagent was prepared from equivalent amounts of 0.1% N-(1-naphthyl) ethylenediamine dihydrochloride and 1% sulphanilamide generated in 2.5% phosphoric acid. For this test, 500 µL of 10 mM sodium nitroprusside in phosphate-buffered saline (pH 7.4) and 1 mL of the SNPs at various concentrations

(50–300 µg/mL) were incubated for 150 min at 25 °C. Then, 1.5 mL of freshly made Griess reagent was added to the product solution after the incubation period. The combination's absorbance was then measured at 546 nm. The control and standard samples were made in the same way as the test samples by using buffer and Trolox instead of the SNPs. The ability of each extract to remove nitric oxide was evaluated [49]. The IC_{50} value is the concentration of the tested drug required to scavenge 50% of the nitric oxide radicals.

2.7. Inhibition of Protein Denaturation

The SNPs were examined for their influence on protein denaturation using the method published by Hmidani et al. [50] with the SNPs (1 mL) at various concentrations (50–300 µg/mL) and 1 mL 1% bovine albumin produced in phosphate-buffered saline (PBS, pH 6.4). The reaction mixtures were kept at 37 °C for 20 min and then heated to 70 °C for 5 min in a shaking water bath. After cooling, the turbidity of the reaction mixture was evaluated at 660 nm. The control and standard samples were produced similarly to the test samples, but they included buffer and diclofenac sodium (50–300 µg/mL) rather than the SNPs. According to Vijayakumar et al [51] findings, the percentage of inhibition of protein denaturation (% IPD) was calculated.

2.8. Cytotoxicity Assessment

Following treatment, to assess the substance's cytotoxicity, the Alomar blue test was employed on tumor and non-tumor cells, as reported by Ahmed et al [52]. On 96-well plates, tumor and non-tumor cells were seeded at a density of 0.7×10^5 cells/mL in 100 µL of complete media. After dissolving the SNPs in 0.5% DMSO, 50 to 300 g/mL was applied to the plates and incubated for 72 h. Following incubation, 20 µL l of Alomar blue stock solution (0.312 mg/mL) was given to each well. Using a microplate reader, the absorbance was measured at a wavelength of 570 nm (Molecular Devices; Sunnyvale, CA, USA). Using duplicate samples, at least three separate experiments were used to confirm each outcome. GraphPad Prism 7.0 (GraphPad Software Inc., La Jolla, CA, USA) was used to estimate the SNPs' half-inhibitory concentrations (IC_{50}).

2.9. Evaluation of SNPs on the Membrane of Guided Tissue Regeneration

Because biodegradable collagen membranes are routinely used for directed tissue regeneration, collagen was chosen as the substrate for nanosilver impregnation. This study used two GTR membranes (Perio Col®- GTR, Educare, Chennai, India): the GTR-C: plain GTR membrane as a negative control; the GTR-NS: GTR membrane impregnated with the SNPs as the test group. The GTR-NS membranes were prepared following the methods described previously [53,54]. Control membranes were frozen after 3 h in distilled water. After the treatment, the membranes turn light to dark yellow. Freeze-drying protects the material's physical structure for storage or transport. Drying nanosilver [55] does not influence the drug release profile or antibacterial action.

For the qualitative assessment of microbial adhesion, membranes were cut into circular pieces 6 mm in diameter in a sterile setting. Membranes were put into Eppendorf tubes holding 2 mL of brain heart infusion broth (BHIB) media. All tubes were horizontally oriented. The tubes were injected with bacterial cultures of the tested oral pathogenic strains (3×10^4 CFU/mL) and incubated at 37 °C. Bacterial adherence to the membranes was assessed after 1, 3, 5, and 7 days following the assessment criteria [56].

Penetrability studies were conducted in a device developed by [8] under a laminar flow hood. Each membrane was placed over an inner glass tube containing the growth material utilized in this investigation for each of the four strains. Silicone O-rings were used to seal the inner glass tubes, then inserted into the outer glass tube (Figure 1). The outer bottle was inoculated with a new culture of oral pathogenic bacterial strains (3×10^4 CFU) in 3 mL of BHIB media, and the devices were incubated in the appropriate atmosphere. The bacterial counts in the inner tubes were determined at certain time intervals (1, 3, 5, and 7 days) using agar plates with the appropriate agar. The presence of colonies in the

outer tube was verified on agar plates to avoid misrepresentative negative and positive findings. On BHI agar plates, colonies of various bacteria were counted.

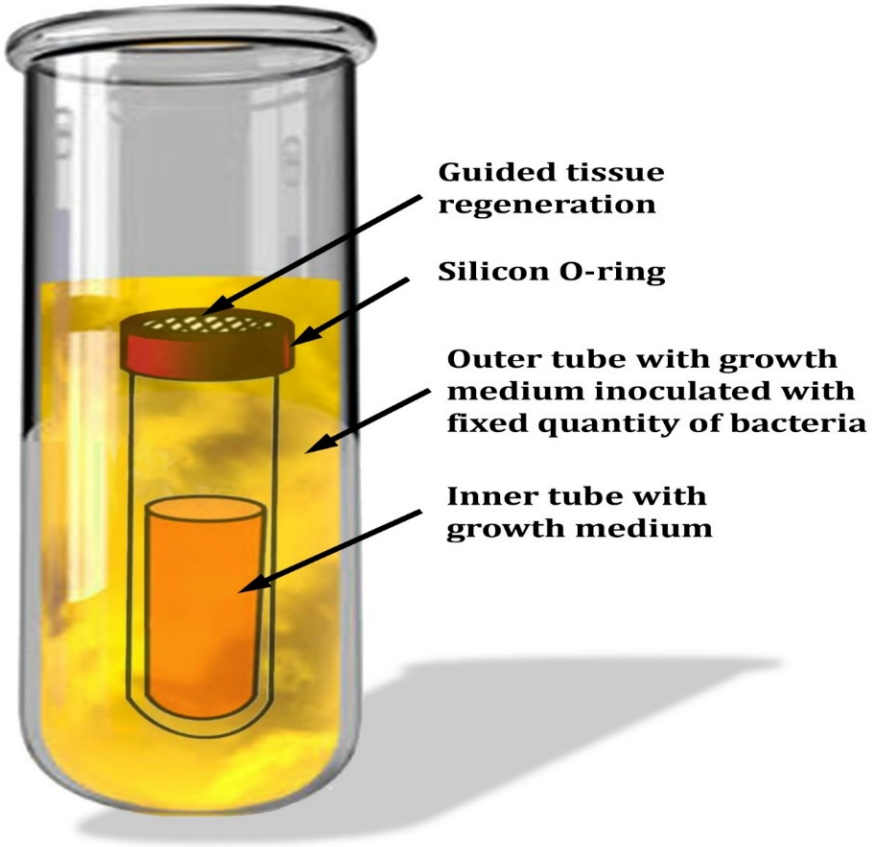

Figure 1. Schematic representation of the in vitro experimental setup for the permeability test of bacteria.

2.10. Statistical Analysis

The data were interpreted using the Minitab statistical software (19.2020.1, Minitab Inc., Chicago, IL, USA). A p-value of <0.05 denotes statistical significance.

3. Results and Discussion

Dentistry faces a significant challenge in oral health management because of the complexity of systems that prevent and control the spread of several microorganisms [57]. Since plaque allows bacteria to colonize teeth and is associated with several oral infectious diseases, plaque is a critical biological habitat [58]. The emergence of antibiotic-resistant bacteria, as well as the increasing frequency of hospital illness outbreaks have rekindled interest in non-pharmaceutical alternatives to synthetic therapies [59,60]. Since SNPs have excellent antibacterial resistance, they have found various applications [61]. The present work attempted to synthesize SNPs in an eco-friendly from an actinobacterium and investigated their biological activities such as antibacterial, antibiofilm, and anti-inflammatory. The actinobacterium isolate used in this study was identified molecularly using 16S rRNA. The MS-37 strain contains 97.62% *Streptomyces rochei*. The BLAST analysis and phylogenetic relationship to *Streptomyces rochei* strain MS-37 revealed a high similarity to the *Streptomyces rochei* SCSIO ZJ89 strain (MF 104551) (Figure 2).

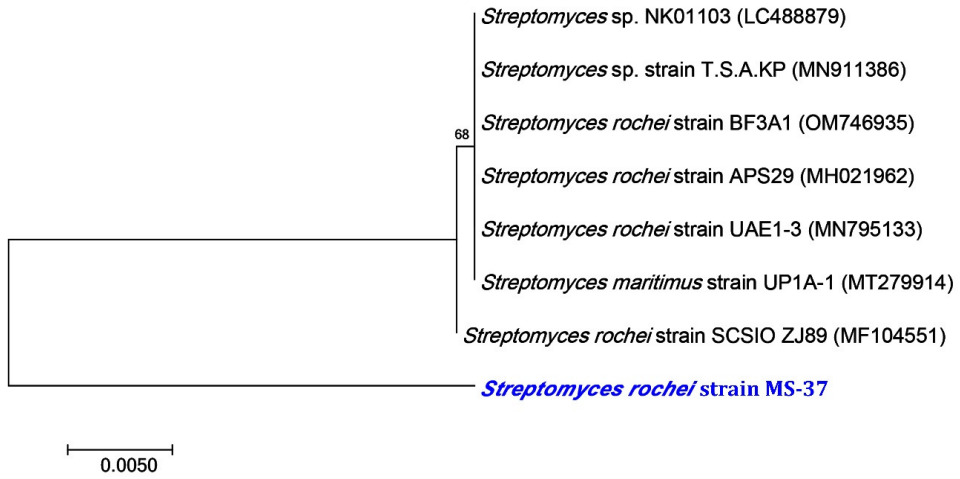

Figure 2. A neighbor-joining tree of *Streptomyces rochei* MS-37 with its closely related taxa. The bootstrap consensus tree inferred from 1000 replicates represents the evolutionary history of the taxa analyzed. The scale bar indicates 0.005 substitutions per nucleotide position.

The SNPs were identified and characterized using UV-Vis spectroscopy. In the reaction mixture, the results confirmed the presence of a peak with a maximum absorbance at 428 nm (Figure 3), which falls within the wavelength range recommended for SNPs and, thus, demonstrated their presence [22]. Additionally, various investigations revealed that SNPs were typically detected using UV-Vis spectroscopy, with peaks spanning 420 to 450 nm [62,63]. The SNPs were also spherical and polydispersed, with sizes ranging from 15–35 nm (mean size = 23.2 nm), as shown in Figure 4A,B, which was obtained using transmission electron microscopy. Nanomaterial size is significant because it affects its physical characteristics, cell penetration, and interactions with living cell molecules. Smaller silver nanoparticles have a higher surface area than larger particles when comparing the same amount of material, and their surface activity is higher as well [64]. The smaller the nanoparticles, the easier it is for them to pass through biological membranes and cause damage [7,20,22]. Contradicting the latter, [65,66] showed that gold nanoparticles with a diameter of 50 nm cross the cellular membrane more efficiently than nanoparticles with diameters of 30 nm and 14 nm, respectively, and [66] showed that gold nanostars with a total encumbrance of 75 nm enter cells better than nanoparticles with a diameter of 45 nm.

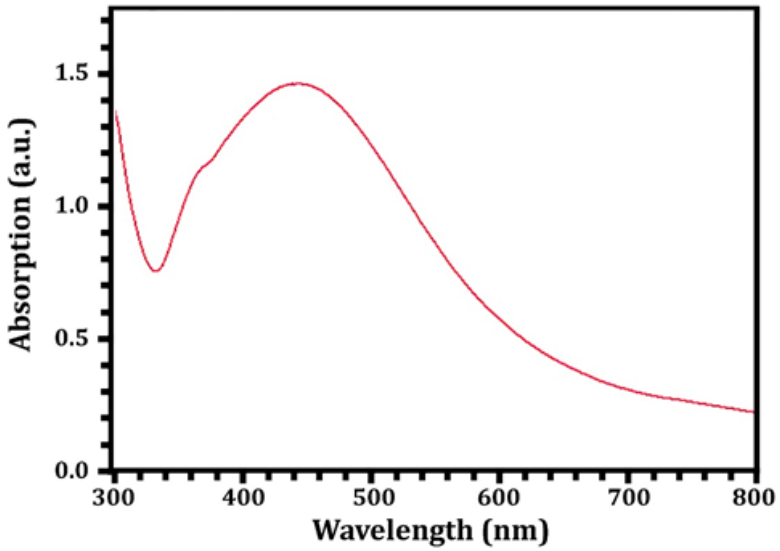

Figure 3. UV-Vis spectra of the *Streptomyces rochei* MS-37-derived SNPs.

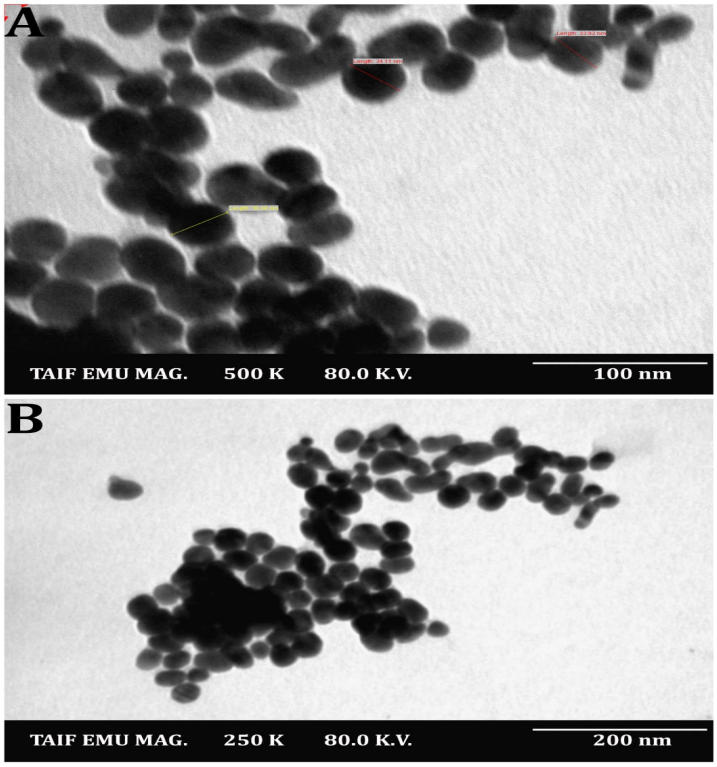

Figure 4. TEM images of the *Streptomyces rochei* MS 37-derived SNPs. Magnification power at 100 nm (**A**) and at 200 nm (**B**).

FTIR analysis was used to identify the biomolecules participating in the reduction of silver ions (Ag^+) and the capping of the resulting SNPs. The FTIR spectra of the SNPs had six absorbance bands; 3400, 2925, 1640, 1385, 1013, and 690 cm^{-1} (Figure 5). The peak at 3400 cm^{-1} is attributed to the stretching vibrations of O-H bonds in alcohols and phenols [67]. The band at 2925 cm^{-1} (C–H stretch) belongs to the alkanes group, but the peak at 1640 cm^{-1} belongs to the N-H bend of primary amines [68]. The peak at 1385 cm^{-1} is attributed to symmetrical carboxyl group stretching [69]. The 1013 cm^{-1} band is related to the C–N stretching vibrations of aromatic and aliphatic amines [70]. FTIR data clearly demonstrated the presence of phenolic compounds and proteins that are likely engaged in the SNPs, as well as the potential that proteins play a significant role in the stabilization of the SNPs by capping, which inhibits agglomeration and helps to strengthen the stability of the SNPs [38].

In view of the fact that TEM images are captured using a dry sample and a high vacuum, additional DLS experiments were performed to determine the particle size in aqueous or physiological conditions. Therefore, DLS and Zeta were used to determine the particle size and potential stability of the SNPs. The SNPs had a particle size of 59.4 mm (Figure 6) and a Zeta potential of −26 mV (Figure 7), according to the obtained results. The SNPs had a particle size of 59.4 nanometers, which is somewhat larger than the particle size identified by TEM, likely owing to Brownian motion. Due to their encapsulation in an organic layer, the nanoparticles did not aggregate despite the fact that the SNPs agglomerated. Consequently, the size difference between the biosynthesized SNPs measured by TEM (23.2 nm) and DLS (59.4 nm) may be attributed to the fact that the two methods are based on fundamentally different physical principles. TEM analysis identifies the diameter of dried particles and the diameter of their metallic core, while DLS analysis measures the hydrodynamic radius of nanoparticles in solution, and the resultant nanoparticle size is always larger [71].

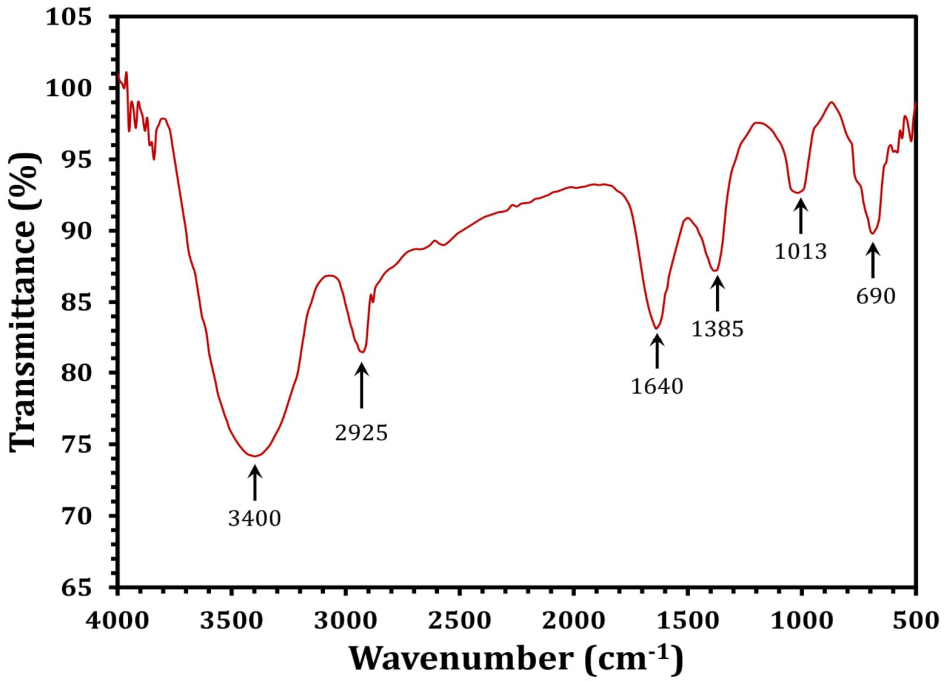

Figure 5. FTIR spectra of the *Streptomyces rochei* MS-37-derived SNPs.

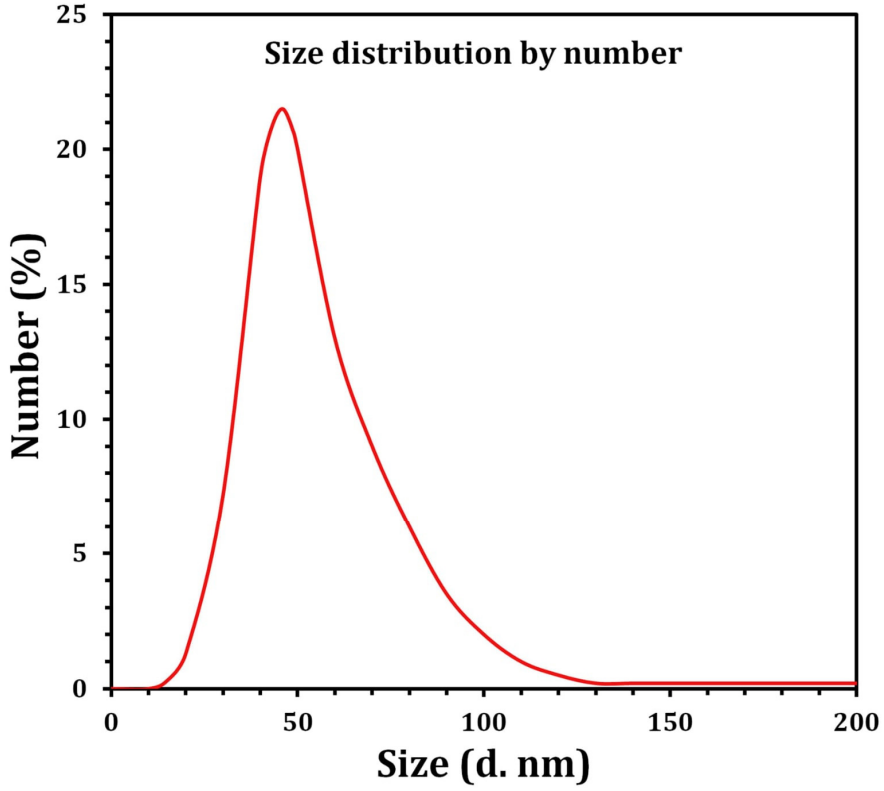

Figure 6. Size distribution by the number graph of the SNPs as revealed by DLS.

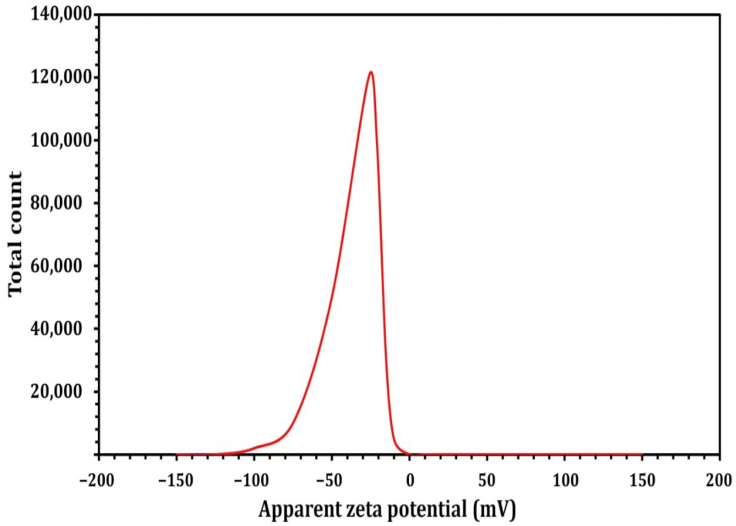

Figure 7. Zeta potential result of the *Streptomyces rochei* MS- 37 SNPs.

In most cases, bacteria that prevent the formation of periodontal pockets are the cause of periodontal infections [5]. Microbes thrive in periodontal pockets because they provide an ideal environment for them to survive and grow [72]. Dental cleanliness, pocket depth, the flow of gingival crevice fluid, gingivitis severity, type of interacting bacteria and viruses, host immune response, emerging pathogens, and antibiotic resistance all have an impact on the quantity and variety of microorganisms in the mouth [73]. As a result of their low cost and high effectiveness, antibiotics have traditionally been used to treat bacterial infection [55]. Several studies have found that widespread antibiotic use has resulted in the emergence of multidrug-resistant (MDR) bacterial strains. Clearly, antibiotic overuse has recently resulted in the emergence of MDR to nearly all antibiotics [21,74]. As a result, novel antimicrobial agents that are highly effective, non-invasive, non-toxic, and drug-resistant are required [75]. Surprisingly, nanoparticles are being evaluated as a possible alternative to antibiotics, and they appear to offer substantial promise in the fight against microbial MDR [18,76]. In light of this, gingival bacterial pathogens were isolated, and their antibiotic susceptibility was determined from the oral cavity of affected individuals. Additionally, the antibacterial efficacy of the SNPs produced was examined. The oral clinical isolates recognized the partial 16S rRNA gene sequence (continuous stretches of approximately 700–1145 bp). The resulting partial 16S rRNA gene sequences were deposited in the EMBL database. The bacteria isolated were identified as *Staphylococcus aureus* M0601, *Staphylococcus aureus* M0901, *Staphylococcus aureus* M1102, *Staphylococcus epidermidis* M0201, and *Staphylococcus hominis* M0401, using the accession codes shown in Table 1.

Table 1. Molecular identification of oral cavity bacterial species based on GeneBank BLAST comparisons.

Strain No.	Nomenclature	Accession No.	Closest Relative Yeast	Sequence Identity (%)
M0601	*Staphylococcus aureus*	LN899797	*Staphylococcus aureus* strain WO53 (LC107797)	100.0
M0901	*Staphylococcus aureus*	LN899798	*Staphylococcus aureus* strain GR41 (LC107809)	99.57
M1102	*Staphylococcus aureus*	LN899800	*Staphylococcus aureus* isolate H3 (LN899816)	99.90
M0201	*Staphylococcus epidermidis*	LN899795	*Staphylococcus epidermidis* strain TMPC 9023C (OM265429)	100.0
M0401	*Staphylococcus hominis*	LN899796	*Staphylococcus hominis* strain PL562 (MK015863)	99.68

Various studies have shown that pathogenic bacteria acquired defense strategies that made them more difficult to treat, such as resistance genes or genetic alterations, resulting

in extended infection with a greater mortality rate [4,75,77]. Nosocomial diseases have evolved from easily treated bacteria to highly resistant bacteria due to the widespread use of antimicrobial drugs. This shift presents a significant challenge for nosocomial infection control and prevention [21,78]. The term MDR bacteria refers to bacteria resistance to many antibiotics that they would ordinarily be sensitive to or to all antibiotic classes except for one or two [79]. Herein, the antibiotic susceptibility patterns of the selected bacteria were studied using the disc diffusion method, as detailed in Table 2. *S. hominis* M0401 and *S. epidermidis* M0201 showed the greatest antibiotic resistance patterns assessed. In addition, all isolates had a higher prevalence of MDR (n = 5−13) [21,74,78]. Interestingly, nanoparticles are now being evaluated as a possible alternative to antibiotics, and they appear to offer substantial promise in the fight against microbial MDR [18,76]. SNPs are a significant metallic nanoscale substance with significant antibacterial activity against various pathogens, including oral bacteria [20]. In this experiment, the biosynthesized SNPs showed an antibacterial impact against oral pathogenic bacteria, as revealed in Table 2. All bacterial isolates were highly sensitive to the SNPs, with MIC values ranging from 8 to 128 µg/mL. *S. epidermidis* M0201 was significantly less sensitive to the SNPs tested (MIC = 128 µg/mL and MBC = 256 µg/mL) than *S. aureus* M1102, *S. aureus* M0601, *S. aureus* M0901, and *S. hominis* M0401 (MIC values of 8, 16, 64, and 64 µg/mL, respectively; MBC values of 32, 32, 64, and 128). While SNPs' antibacterial mechanisms of action have been widely studied and disputed, they are still not completely understood. SNPs have two well-established antibacterial mechanisms: direct and ion-mediated degradation [80]. When bacteria are exposed to SNPs, the nanoparticles bind to the cell wall's surface [81]. SNPs have significant potential for efficiency enhancement by optimizing their physicochemical properties, also leading to a rise in the ability of bacteria's macromolecules with functionalized sulfur and phosphorous to attach, causing cell death [82,83]. As a result, SNPs degrade the lipid bilayer's integrity and the accessibility of the cytoplasmic membrane, as these are essential for the proper transport regulation via the cytoplasmic membrane [84,85]. Furthermore, SNPs' antibacterial action produces a high amount of reactive oxygen and free radical species that prevent cell respiration and reproduction [86,87].

Table 2. Antimicrobial activity of the SNPs against periodontal pathogenic strains.

Periodontal Pathogens	Antibiotic Resistance Pattern	[#] SNPs (µg/mL)	
		MIC	MBC
S. aureus M1102	VA, E, PB, OX, CAZ	8	32
S. aureus M0601	TE, VA, E, PB, AMC, OX, FOX	16	32
S. aureus M0901	VA, GN, NOR, E, PB, AMC, OX, FOX, CAZ	64	64
S. hominis M0401	TE, VA, GN, CIP, NOR, E, C, PB, AMC, OX, CAZ	64	128
S. epidermidis M0201	TE, VA, GN, AK, CIP, NOR, E, C, PB, AMC, OX, FOX, CAZ	128	256

TE, Tetracyclines; **VA**, Vancomycin; **GN**, Gentamicin; **AK**, Amikacin; **CIP**, Ciprofloxacin; **NOR**, Norfloxacin; **E**, Erythromycin; **C**, Chloramphenicol; **PB**, Polymyxin B; **AMC**, Amoxicillin-clavulanic acid; **OX**, Oxacillin; **FOX**, Cefoxitin; **CAZ**, Ceftazidime. [#] **SNPs**, silver nanoparticles; **MIC**, minimum inhibitory concentration; **MBC**, minimum bactericidal concentration.

Furthermore, nanoparticles' biocidal effects are aided by the silver ions they produce [88,89]. They might also affect potassium ion release and transit across microbial cell membranes. Ions, proteins, reducing sugars, and adenosine triphosphate are examples of cellular constituents (ATP), the cell's energy reserve, leaking out of the cell due to the membrane's increased permeability [90–92]. SNPs and/or silver ions can interact with biological components such as ribosomes and macromolecules including proteins, lipids, and DNA in microbial cells, killing the organisms. They prevent the function of proteins, the translation of ribosomes, and DNA replication [88,93].

Antibiotic resistance is often prevalent at a high to moderate level, resulting from their biofilm-forming ability [94]. As a result, inquiries into the pathogenesis of these diseases have concentrated on the method by which these microbes adhere to the collected specimens. Their high incidence of antibiotic resistance may result from their ability to form biofilms. All isolated *Staphylococcus* spp. could form a biofilm on polystyrene surfaces, although in various patterns (Table 3). *S. aureus* strains M1102, *S. hominis* M0401, and *S. epidermidis* M0201 are strong biofilm producers (+++), but *S. aureus* M0901 exhibits a moderate ability to form a biofilm (++), while *S. aureus* M0601 is a weak biofilm producer (+). Regarding antibiofilm activity, SNP treatment had a significant effect on the majority of strains, lowering their ability to form biofilms from strong (+++) to non-producing (-). On the other hand, the SNPs had no influence on *S. epidermidis* M0201 adherence to biofilms (Table 3). It is reported that strain-dependent inhibition of staphylococcal biofilm formation was detected when the culture media was supplemented with the SNPs. Additionally, these biosynthesized SNPs had significant antibiofilm action against pathogenic bacteria related to gingival disease.

Table 3. Quantitative detection of biofilm formation by Staphylococcus sp. using the MtP assay.

Bacterial Strain	Biofilm Formation before Treatment		Biofilm Formation after Treatment with SNPs	
	Producing Category	A_{630nm}	Producing Category	A_{630nm}
S. aureus M1102	+++	0.272 ± 0.00	-	0.10 ± 0.002
S. aureus M0601	+	0.110 ± 0.01	-	0.08 ± 0.003
S. aureus M0901	++	0.210 ± 0.01	-	0.07 ± 0.004
S. hominis M0401	+++	0.255 ± 0.00	-	0.11 ± 0.001
S. epidermidis M0201	+++	0.56 ± 0.02	+++	0.45 ± 0.002

-, not a producer; +, weak; ++, moderate; +++, strong biofilm producer.

Inflammation is a physiological response to potentially harmful stimuli such as irritants, damaged cells, or infection [11]. Systemic or localized inflammation can be acute or chronic [12]. To protect cells and tissues during the acute inflammatory process, different immune cells or neutrophil respiratory bursts produce a wide range of mediators, including prostaglandins, cytokines, and other ROSs, such as nitric oxide (NO) [12]. The antioxidant activity of standard Trolox and the SNPs was evaluated using a nitric oxide radical scavenging test, with IC_{50} values of 110.7 ± 6.15 and 80.07 ± 4.2 µg/mL, respectively (Table 4). The SNPs may be essential in minimizing the adverse effects of excessive NO creation in the human body since they can reduce NO production. Additionally, the scavenging activity might obstruct the series of negative effects brought on by excessive NO creation [95]. Increased vascular permeability, protein denaturation, and membrane alteration are just a few of the many processes that contribute to inflammation, which frequently causes modification. Denaturation occurs when proteins lose their tertiary and secondary structures due to stress or heat. The IC_{50} values for diclofenac sodium and the SNPs were determined to be 215.5 ± 4.90 µg/mL and 189.44 ± 5.52 µg/mL, respectively (Table 4). reported similar findings, which might be explained by the combined impact of bioactive agents adsorbed on the surface of SNPs, which increases their dispersibility and bioavailability [96].

Cytotoxic activity is a critical feature to consider when determining a substance's safety for usage in medical uses. Therefore, to assess the tumor cytotoxicity of the SNPs after 72 h of treatment, a cytotoxicity test using Alomar Blue was performed. The investigation used normal mammalian cells, peripheral blood mononuclear cells (PBMC), and an oral adenosquamous carcinoma cell line (CAL27). The SNPs had an IC_{50} of 81.16 µg/mL in PBMCs and 34.03 µg/mL in CAL27 (Table 4). The toxicity of the SNPs in PMBCs may be attributed to the release of free silver ions, the total silver ion concentration, or the interaction of cellular components with the nanoparticles. Furthermore, SNPs have

demonstrated a range of cytotoxic effects in several cell types, indicating that they impair cell viability by interfering with mitochondrial structure and metabolism [62].

Table 4. Effect of the SNPs on nitric oxide radical scavenging activity, protein denaturation inhibition, and cytotoxicity (µg/mL).

Tested Materials	IC_{50} (µg/mL)			
	Nitric Oxide Radical Scavenging Activity	Inhibition of Protein Denaturation	* Cytotoxicity	
			CAL27	PMBC
SNPs	110.7 ± 6.15	89.44 ± 5.52	34.03	81.16
Standard	80.07 ± 4.2 #	215.5 ± 4.90 ##	-	-

The data are provided as IC_{50} values in µg/mL with a 95% confidence interval derived from at least three independent tests conducted in duplicate. * Cytotoxicity was determined 72 h after treatment using the Alamar Blue test. SNPs, silver nanoparticles; CAL27, oral adenosquamous carcinoma cell lines; PMBC, human peripheral blood mononuclear cells. # Trolox; ## diclofenac sodium.

The adhesion and penetration of the chosen strains into their corresponding membrane groups were tested in this investigation during four-time intervals. As shown in Table 5, the mean adherence score increased significantly at the end of Days 3, 5, and 7 for the two groups compared to Day 1 ($p = 0.001$). The SNPs significantly reduced *S. epidermidis* M0201 adhesion to the membrane in GTR-NS, reaching a maximum of 1.8 ± 0.43 after day 7, compared to 3.3 ± 0.21 for GTR-C, a difference of $p = 0.001$. The mean bacterial adherence scores were significantly higher in the GTR-C group than in the GTR-NS group throughout various incubation times and bacterial strains. This difference was statistically significant with respect to the adherence scores ($p = 0.001$). This experiment employed collagen membranes as the substrate for silver nanoparticle deposition. Bacterial adhesion is observed to decrease when the hydrophobicity of biomaterials rises [19,23]. Due to its greater hydrophilicity, collagen is more susceptible to bacterial colonization by *S. mutans*, *A. actinomycete mcomitans*, *F. nucleatum*, and *P. gingivalis* than other GTR membranes [8]. Collagen is a viscoelastic substance with a high tensile strength, but limited elasticity [96] or loading with other nanoparticles may affect their fundamental physical characteristics [97,98]. The mean CFUs cultivated from the inner tube were used to determine bacterial penetration across the GTR membranes (Table 6). The number of CFU/mL cultured from the inner tube on Days 3, 5, and 7 was contrasted with the number of CFU/mL cultured from the inner tube on one day. In terms of penetration for all examined bacteria, the mean CFUs grown from the inner tube were higher in the GTR-C group than in the GTR-NS group at all incubation intervals. The number of CFU/mL cultivated from the inner tube significantly decreased (P 0.001) on Days 3, 5, and 7 in the GTR-NS group, *S. aureus* M1102, M0601, and M0901. Additionally, no growth was seen in the inner tube culture of *S. hominis* M0401 or *S. epidermidis* M0201 (Table 6). A GTR membrane that is medically controllable must be both rigid and elastic [97]. Suppose SNPs-coated GTR membranes are approved for intraoral clinical use. In that case, it will be intriguing to observe how the change in mechanical characteristics impacts clinical manageability, space formation, and, eventually, the possibility of periodontal regeneration [7].

Table 5. Qualitative assessment of bacterial adherence.

Group	Day	Adherence Score				
		S. aureus **M1102**	***S. aureus*** **M0601**	***S. aureus*** **M0901**	***S. hominis*** **M0401**	***S. epidermidis*** **M0201**
GTR-C	1	1.1 ± 0.3	1.0 ± 0.0	1.1 ± 0.34	1.3 ± 0.6	1.4 ± 0.8
	3	1.99 ± 0.33 *	1.1 ± 0.3	1.2 ± 0.24	1.5 ± 0.5	2.05 ± 0.2 *
	5	2.04 ± 0.24 *	2.2 ± 0.45 *	2.14 ± 0.4 *	3.0 ± 0.24 *	3.1 ± 0.3 *
	7	2.9 ± 0.3 *	3.2 ± 0.1 *	2.95 ± 0.23 *	3.1 ± 0.1 *	3.3 ± 0.21 *
GTR-NS	1	0.08 ± 0.1	0.05 ± 0.01	0.08 ± 0.04	0.9 ± 0.1	1.0 ± 0.02
	3	1.0 ± 0.2 *	1.1 ± 0.4 *	1.3 ± 0.5 *	1.3 ± 0.5 *	1.4 ± 0.3 *
	5	1.5 ± 0.3 *	1.4 ± 0.6 *	1.6 ± 0.4 *	1.4 ± 0.2 *	1.6 ± 0.4 *
	7	1.8 ± 0.8 *	1.5 ± 0.72 *	1.7 ± 0.48 *	1.5 ± 0.5 *	1.8 ± 0.43 *

* Highly significant as compared to the levels at Day 1 using the Tukey HSD/multiple comparisons. Values are the mean of the triplicate ± SD. GTR, guided tissue regeneration; C, control; NS, nanosilver. p-value < 0.05 is considered significant.

Table 6. Bacterial penetration of control (GTR-C) and silver-nanoparticle (GTR-NS)-impregnated collagen guided tissue regeneration (GTR) membranes.

Group	Day	CFU/mL				
		S. aureus **M1102**	***S. aureus*** **M0601**	***S. aureus*** **M0901**	***S. hominis*** **M0401**	***S. epidermidis*** **M0201**
GTR-C	1	285.2 ± 3.0	125.0 ± 0.0	95.1 ± 0.0	121.17 ± 3.8	160.4 ± 0.8
	3	255.5 ± 2.9 *	155.58 ± 0.3	198.6 ± 1.2	199.8 ± 1.6	210.2 ± 0.2 *
	5	240.1 ± 0.24 *	278.2 ± 8.45 *	198.8 ± 0.4 *	235.17 ± 6.24 *	270.0 ± 5.3 *
	7	179.58 ± 7.3 *	269.4 ± 4.51 *	300.0 ± 3.3 *	285.2 ± 3.1 *	330 ± 4.81 *
GTR-NS	1	146.78 ± 8.1	99.0 ± 0.1	82.7 ± 1.4	90.0 ± 8.1	100.0 ± 7. 2
	3	126.54 ± 9.2 *	84.9 ± 3.4 *	71.2 ± 6.5 *	71.2 ± 4.5 *	94.2 ± 5.3 *
	5	115.0 ± 0.3 *	70.0 ± 6.6 *	51.4 ± 4.4 *	54.0 ± 2.2 *	46.0 ± 4.4 *
	7	74.47 ± 10.8 *	40.8 ± 7.72 *	32.17 ± 6.8 *	0.0 ± 0.0 *	0.0 ± 0.0

* Values are the mean of the triplicate ± SD. p-value < 0.05 is considered significant.

4. Conclusions

The findings of this work provide a new path for the application of marine-derived SNPs, which demonstrated outstanding antibacterial activity against clinically isolated oral biofilms from gingivitis specimens. Studies indicate that SNPs have anti-inflammatory effects by preventing protein denaturation and using nitric oxide to scavenge free radicals. While the present study's in vitro results on the CAL27 cell line are encouraging, the efficacy of SNPs with known effects on viability should be investigated in vivo. This information will be critical for pre-clinical studies examining the therapeutic potential of SNPs in gingivitis therapies.

Author Contributions: Conceptualization, S.E.E., M.A.K. and T.A.A.; methodology, S.E.E., M.A.K., T.A.A. and F.A.A.; software, S.S.A.; validation, S.E.E., M.A.K. and T.A.A.; formal analysis, S.E.E. and S.S.A.; investigation, M.A.K. and T.A.A.; resources, S.E.E., M.A.K., T.A.A. and S.S.A.; data curation, S.E.E.; writing—original draft preparation, F.A.A. and T.A.A.; writing—review and editing, S.E.E., M.A.K. and S.S.A.; visualization, F.A.A. and T.A.A.; supervision, S.E.E., M.A.K. and T.A.A.; project administration, M.A.K. and T.A.A.; funding acquisition, M.A.K. All authors have read and agreed to the published version of the manuscript.

Funding: This work was supported by Taif University Researchers Supporting Project Number TURSP-2020/95, Taif University, Taif, Saudi Arabia.

Institutional Review Board Statement: All samples were kindly provided from the dental clinics in Taif city during January 2017 till July 2017.

Informed Consent Statement: Not applicable.

Data Availability Statement: This article has all the data that were created or evaluated during this investigation.

Conflicts of Interest: The authors declare no conflict of interest.

Sample Availability: Samples of the compounds are available from the authors.

References

1. AlJasser, R.; AlAqeely, R.; AlKenani, M.; AlQahtani, S.; AlZahrani, A.; Lambarte, R. The effect of systemic Isotretinoin on salivary tissue inhibitors of metalloproteinases 1 and 2 and salivary flow rate in periodontal disease. *Saudi J. Biol. Sci.* **2022**, *29*, 148–153. [CrossRef]
2. Yadalam, P.K.; Rengaraj, S.; Mugri, M.H.; Sayed, M.; Porwal, A.; Alahmari, N.M.; Alzahrani, K.M.; Robaian, A.; Baeshen, H.A.; Patil, S. Designing an immunoinformatic vaccine for peri-implantitis using a structural biology approach. *Saudi J. Biol. Sci.* **2022**, *29*, 622–629. [CrossRef] [PubMed]
3. Johansson, I.; Witkowska, E.; Kaveh, B.; Lif Holgerson, P.; Tanner, A.C.R. The microbiome in populations with a low and high prevalence of caries. *J. Dent. Res.* **2016**, *95*, 80–86. [CrossRef] [PubMed]
4. Khalil, M.; El-Sabbagh, M.; El Naggar, E.; El-Erian, R. Antibacterial activity of *Salvadora persica* against oral pathogenic bacterial isolates. *Niger. J. Clin. Pract.* **2019**, *22*, 1378–1387. [CrossRef]
5. Bhatia, A.; Bains, S.K.; Singh, M.P. To assess knowledge and awareness of North Indian population towards periodontal therapy and oral-systemic disease link: A cross-sectional survey. *J. Interdiscip. Dent.* **2013**, *3*, 79. [CrossRef]
6. Moghadam, E.T.; Yazdanian, M.; Tahmasebi, E.; Tebyanian, H.; Ranjbar, R.; Yazdanian, A.; Seifalian, A.; Tafazoli, A. Current herbal medicine as an alternative treatment in dentistry: In vitro, in vivo and clinical studies. *Eur. J. Pharmacol.* **2020**, *889*, 173665. [CrossRef] [PubMed]
7. Rani, S.; Chandra, R.V.; Reddy, A.; Reddy, B.; Nagarajan, S.; Naveen, A. Evaluation of the antibacterial effect of silver nanoparticles on guided tissue regeneration membrane colonization—An in vitro study. *J. Int. Acad. Periodontol.* **2015**, *17*, 66–76. [PubMed]
8. Rossa, M.L.; Lima, L.A.; Pustiglioni, F.E.; Hespanhol, A.M.; Kon, S.; Grigolli Filho, J. SEM analyses of bacterial contamination of e-PTFE membranes and GTR clinical results. *J. Inter. Acad. Periodontol.* **2006**, *8*, 115–124.
9. Cheng, C.F.; Lee, Y.Y.; Chi, L.Y.; Chen, Y.T.; Hung, S.L.; Ling, L.J. Bacterial penetration through antibiotic-loaded guided tissue regeneration membranes. *J. Periodontol.* **2009**, *80*, 1471–1478. [CrossRef]
10. Wang, Z.; Liu, X.; Duan, Y.; Huang, Y. Infection microenvironment-related antibacterial nanotherapeutic strategies. *Biomaterials* **2021**, *280*, 121249. [CrossRef]
11. Wei, Y.; Yang, L.; Pandeya, A.; Cui, J.; Zhang, Y.; Li, Z. Pyroptosis-induced inflammation and tissue damage. *J. Mol. Biol.* **2021**, *434*, 167301. [CrossRef] [PubMed]
12. Zhang, H.; Tsao, R. Dietary polyphenols, oxidative stress and antioxidant and anti-inflammatory effects. *Curr. Opin. Food Sci.* **2016**, *8*, 33–42. [CrossRef]
13. Ahamad, N.; Kar, A.; Mehta, S.; Dewani, M.; Ravichandran, V.; Bhardwaj, P.; Sharma, S.; Banerjee, R. Immunomodulatory nanosystems for treating inflammatory diseases. *Biomaterials* **2021**, *274*, 120875. [CrossRef]
14. Elisha, I.L.; Dzoyem, J.P.; McGaw, L.J.; Botha, F.S.; Eloff, J.N. The anti-arthritic, anti-inflammatory, antioxidant activity and relationships with total phenolics and total flavonoids of nine South African plants used traditionally to treat arthritis. *BMC Complement. Altern. Med.* **2016**, *16*, 307. [CrossRef] [PubMed]
15. Ali, S.S.; Morsy, R.; El-Zawawy, N.A.; Fareed, M.F.; Bedaiwy, M.Y. Synthesized zinc peroxide nanoparticles (ZnO_2-NPs): A novel antimicrobial, anti-elastase, anti-keratinase, and anti-inflammatory approach toward polymicrobial burn wounds. *Int. J. Nanomed.* **2017**, *12*, 6059. [CrossRef]
16. Ali, S.S.; Sonbol, F.I.; Sun, J.; Hussein, M.A.; Hafez, A.E.E.; Abdelkarim, E.A.; Kornaros, M.; Ali, A.; Azab, M. Molecular characterization of virulence and drug resistance genes-producing *Escherichia coli* isolated from chicken meat: Metal oxide nanoparticles as novel antibacterial agents. *Microb. Pathog.* **2020**, *143*, 104164. [CrossRef]
17. Ali, S.S.; Al-Tohamy, R.; Koutra, E.; Moawad, M.S.; Kornaros, M.; Mustafa, A.M.; Mahmoud, Y.A.G.; Badr, A.; Osman, M.E.; Elsamahy, T.; et al. Nanobiotechnological advancements in agriculture and food industry: Applications, nanotoxicity, and future perspectives. *Sci. Total Environ.* **2021**, *792*, 148359. [CrossRef]
18. Ali, S.S.; Moawad, M.S.; Hussein, M.A.; Azab, M.; Abdelkarim, E.A.; Badr, A.; Sun, J.; Khalil, M. Efficacy of metal oxide nanoparticles as novel antimicrobial agents against multi-drug and multi-virulent *Staphylococcus aureus* isolates from retail raw chicken meat and giblets. *Int. J. Food Microbiol.* **2021**, *344*, 109116. [CrossRef]
19. Khalil, M.A.; El-Shanshoury, A.E.; Alghamdi, M.A.; Mohamed, S.F.; Sun, J.; Ali, S.S. Biosynthesis of silver nanoparticles by marine actinobacterium *Nocardiopsis dassonvillei* and exploring their therapeutic potentials. *Front. Microbiol.* **2022**, *12*, 705673. [CrossRef]
20. Halkai, K.R.; Halkai, R.; Mudda, J.A.; Shivanna, V.; Rathod, V. Antibiofilm efficacy of biosynthesized silver nanoparticles against endodontic-periodontal pathogens: An in vitro study. *J. Conserv. Dent.* **2018**, *21*, 662. [CrossRef]
21. Khalil, M.A.; El Maghraby, G.M.; Sonbol, F.I.; Allam, N.G.; Ateya, P.S.; Ali, S.S. Enhanced efficacy of some antibiotics in presence of silver nanoparticles against Multidrug resistant *Pseudomonas aeruginosa* recovered from burn wound infections. *Front. Microbiol.* **2021**, *12*, 648560. [CrossRef] [PubMed]
22. Khalil, M.A.; Sonbol, F.I.; Al-Madboly, L.A.; Aboshady, T.A.; Alqurashi, A.S.; Ali, S.S. Exploring the therapeutic potentials of exopolysaccharides derived from lactic acid bacteria and bifidobacteria: Antioxidant, antitumor, and periodontal regeneration. *Front. Microbiol.* **2022**, *13*, 803688. [CrossRef] [PubMed]
23. Ong, W.T.J.; Nyam, K.L. Evaluation of silver nanoparticles in cosmeceutical and potential biosafety complications. *Saudi J. Biol. Sci.* **2022**, *29*, 2085–2094. [CrossRef] [PubMed]

24. Panpaliya, N.P.; Dahake, P.T.; Kale, Y.J.; Dadpe, M.V.; Kendre, S.B.; Siddiqi, A.G.; Maggavi, U.R. In vitro evaluation of antimicrobial property of silver nanoparticles and chlorhexidine against five different oral pathogenic bacteria. *Saudi Dent. J.* **2019**, *31*, 76–83. [CrossRef] [PubMed]
25. Sánchez-López, E.; Gomes, D.; Esteruelas, G.; Bonilla, L.; Lopez-Machado, A.L.; Galindo, R.; Cano, A.; Espina, M.; Ettcheto, M.; Camins, A.; et al. Metal-based nanoparticles as antimicrobial agents: An overview. *Nanomaterials* **2020**, *10*, 292. [CrossRef] [PubMed]
26. Bertoglio, F.; De Vita, L.; D'Agostino, A.; Fernandez, Y.D.; Falqui, A.; Casu, A.; Merli, D.; Milanese, C.; Rossi, S.; Taglietti, A.; et al. Increased antibacterial and antibiofilm properties of silver nanoparticles using silver fluoride as precursor. *Molecules* **2020**, *25*, 3494. [CrossRef]
27. Di Federico, A.; Rizzo, A.; Carloni, R.; De Giglio, A.; Bruno, R.; Ricci, D.; Brandi, G. Atezolizumab-bevacizumab plus Y-90 TARE for the treatment of hepatocellular carcinoma: Preclinical rationale and ongoing clinical trials. *Expert Opin. Investig. Drugs* **2022**, *31*, 361–369. [CrossRef]
28. Bahlol, H.S.; Foda, M.F.; Ma, J.; Han, H. Robust synthesis of size-dispersal triangular silver nanoprisms via chemical reduction route and their cytotoxicity. *Nanomaterials* **2019**, *9*, 674. [CrossRef] [PubMed]
29. Veeraraghavan, V.P.; Periadurai, N.D.; Karunakaran, T.; Hussain, S.; Surapaneni, K.M.; Jiao, X. Green synthesis of silver nanoparticles from aqueous extract of *Scutellaria barbata* and coating on the cotton fabric for antimicrobial applications and wound healing activity in fibroblast cells (L929). *Saudi J. Biol. Sci.* **2021**, *28*, 3633–3640. [CrossRef]
30. Suriyakala, G.; Sathiyaraj, S.; Devanesan, S.; AlSalhi, M.S.; Rajasekar, A.; Maruthamuthu, M.K.; Babujanarthanam, R. Phytosynthesis of silver nanoparticles from *Jatropha integerrima* Jacq. flower extract and their possible applications as antibacterial and antioxidant agent. *Saudi J. Biol. Sci.* **2022**, *29*, 680–688. [CrossRef]
31. Monteiro, D.R.; Gorup, L.F.; Takamiya, A.S.; Ruvollo-Filho, A.C.; de Camargo, E.R.; Barbosa, D.B. The growing importance of materials that prevent microbial adhesion: Antimicrobial effect of medical devices containing silver. *Int. J. Antimicrob. Agents* **2009**, *34*, 103–110. [CrossRef] [PubMed]
32. Sharma, D.; Kanchi, S.; Bisetty, K. Biogenic synthesis of nanoparticles: A review. *Arab. J. Chem.* **2019**, *12*, 3576–3600. [CrossRef]
33. Makvandi, P.; Ghomi, M.; Padil, V.V.; Shalchy, F.; Ashrafizadeh, M.; Askarinejad, S. Biofabricated nanostructures and their composites in regenerative medicine. *ACS Appl. Nano Mater.* **2020**, *3*, 6210–6238. [CrossRef]
34. Darwesh, O.M.; Ali, S.S.; Matter, I.A.; Elsamahy, T. Nanotextiles waste management: Controlling of release and remediation of wastes. In *Nanosensors and Nanodevices for Smart Multifunctional Textiles*; Elsevier: Amsterdam, The Netherlands, 2021; pp. 267–286.
35. Chernousova, S.; Epple, M. Silver as antibacterial agent: Ion, nanoparticle, and metal. *Angew. Chem. Int. Ed.* **2013**, *52*, 1636–1653. [CrossRef] [PubMed]
36. Pallavicini, P.; Dacarro, G.; Taglietti, A. Self-assembled monolayers of silver nanoparticles: From intrinsic to switchable inorganic antibacterial surfaces. *Eur. J. Inorg. Chem.* **2018**, *2018*, 4846–4855. [CrossRef]
37. Pandit, C.; Roy, A.; Ghotekar, S.; Khusro, A.; Islam, M.N.; Emran, T.B.; Lam, S.E.; Khandaker, M.U.; Bradley, D.A. Biological agents for synthesis of nanoparticles and their applications. *J. King Saud Univ. Sci.* **2022**, *34*, 101869. [CrossRef]
38. Mabrouk, M.; Elkhooly, T.A.; Amer, S.K. Actinomycete strain type determines the monodispersity and antibacterial properties of biogenically synthesized silver nanoparticles. *J. Genet. Eng. Biotechnol.* **2021**, *19*, 57. [CrossRef]
39. Mohseni, M.; Norouzi, H.; Hamedi, J.; Roohi, A. Screening of antibacterial producing actinomycetes from sediments of the Caspian Sea. *Int. J. Mol. Cell Med.* **2013**, *2*, 64.
40. Veerasamy, R.; Xin, T.Z.; Gunasagaran, S.; Xiang, T.F.W.; Yang, E.F.C.; Jeyakumar, N.; Dhanaraj, S.A. Biosynthesis of silver nanoparticles using mangosteen leaf extract and evaluation of their antimicrobial activities. *J. Saudi Chem. Soc.* **2011**, *15*, 113–120. [CrossRef]
41. Khalil, M.; Abdelhafez, Y.G.; Atta, H.; Kandeel, A.A. SPECT/CT is equivalent to diffusion-weighted MRI in characterizing equivocal osseous lesions detected by planar bone scintigraphy. *Eur. J. Nuclear Med. Mol. Imaging* **2017**, *44*, S218–S219.
42. Liu, X.; Atwater, M.; Wang, J.; Huo, Q. Extinction coefficient of gold nanoparticles with different sizes and different capping ligands. *Colloids Surf. B* **2007**, *58*, 3–7. [CrossRef] [PubMed]
43. Ali, S.S.; El-Sheekh, M.; Manni, A.; Ruiz, H.A.; Elsamahy, T.; Sun, J.; Schagerl, M. Microalgae-mediated wastewater treatment for biofuels production: A comprehensive review. *Microbiol. Res.* **2022**, *265*, 127187. [CrossRef] [PubMed]
44. Goel, N.; Ahmad, R.; Singh, R.; Sood, S.; Khare, S.K. Biologically synthesized silver nanoparticles by *Streptomyces* sp. EMB24 extracts used against the drug-resistant bacteria. *Bioresour. Technol. Rep.* **2021**, *15*, 100753. [CrossRef]
45. CLSI. *Performance Standards for Antimicrobial Susceptibility Tests*, 13th ed.; CLSI Standard M02; Clinical and Laboratory Standards Institute: Wayne, PA, USA, 2018.
46. Christensen, G.D.; Simpson, W.A.; Younger, J.J.; Baddour, L.M.; Barrett, F.F.; Melton, D.M.; Beachey, E.H. Adherence of coagulase-negative staphylococci to plastic tissue culture plates: A quantitative model for the adherence of staphylococci to medical devices. *J. Clin. Microbiol.* **1985**, *22*, 996–1006. [CrossRef] [PubMed]
47. Stepanovic, S.; Vukovic, D.; DakicSavic, I.B.; Svabic-Vlahovic, M. A modified microtiter-plate for quantification of staphylococcal biofilm formation. *J. Microbiol. Methods* **2000**, *40*, 175–179. [CrossRef]
48. Boora, F.; Chirisa, E.; Mukanganyama, S. Evaluation of nitrite radical scavenging properties of selected Zimbabwean plant extracts and their phytoconstituents. *J. Food Process.* **2014**, *2014*, 918018. [CrossRef]

49. Tonisi, S.; Okaiyeto, K.; Mabinya, L.V.; Okoh, A.I. Evaluation of bioactive compounds, free radical scavenging and anticancer activities of bulb extracts of *Boophone disticha* from Eastern Cape Province, South Africa. *Saudi J. Biol. Sci.* **2020**, *27*, 3559–3569. [CrossRef]
50. Hmidani, A.; Bouhlali, E.D.T.; Khouya, T.; Ramchoun, M.; Filali-Zegzouti, Y.; Alem, C.; Benlyas, M. Antioxidant, anti-inflammatory and anticoagulant activities of three Thymus species grown in southeastern Morocco. *Future J. Pharm. Sci.* **2019**, *5*, 4. [CrossRef]
51. Vijayakumar, N.; Bhuvaneshwari, V.K.; Ayyadurai, G.K.; Jayaprakash, R.; Gopinath, K.; Nicoletti, M.; Alarifi, S.; Govindarajan, M. Green synthesis of zinc oxide nanoparticles using *Anoectochilus elatus*, and their biomedical applications. *Saudi J. Biol. Sci.* **2021**, *29*, 2270–2279. [CrossRef]
52. Ahmed, S.A.; Gogal Jr, R.M.; Walsh, J.E. A new rapid and simple non-radioactive assay to monitor and determine the proliferation of lymphocytes: An alternative to [3H] thymidine incorporation assay. *J. Immunol. Methods* **1994**, *170*, 211–224. [CrossRef]
53. Chang, C.Y.; Yamada, S. Evaluation of the regenerative effect of a 25% doxycycline-loaded biodegradable membrane for guided tissue regeneration. *J. Periodontol.* **2000**, *71*, 1086–1093. [CrossRef] [PubMed]
54. Li, X.; Zhang, M.; Duan, X.; Mujumdar, A. Effect of nano-silver coating on microbial control of microwave-freeze combined dried sea cucumber. *Int. Agrophys.* **2011**, *25*, 181–186.
55. Yazdimamaghani, M.; Vashaee, D.; Assefa, S.; Walker, K.J.; Madihally, S.V.; Köhler, G.A. Hybrid macroporous gelatin/bioactive-glass/nanosilver scaffolds with controlled degradation behavior and antimicrobial activity for bone tissue engineering. *J. Biomed. Nanotechnol.* **2014**, *10*, 911–931. [CrossRef] [PubMed]
56. Wang, L.; Hu, C.; Shao, L. The antimicrobial activity of nanoparticles: Present situation and prospects for the future. *Int. J. Nanomed.* **2017**, *12*, 1227. [CrossRef]
57. Espinosa-Cristóbal, L.F.; Holguín-Meráz, C.; Zaragoza-Contreras, E.A.; Martínez-Martínez, R.E.; Donohue-Cornejo, A.; Loyola-Rodríguez, J.P.; Cuevas-González, J.C.; Reyes-López, S.Y. Antimicrobial and substantivity properties of silver nanoparticles against oral microbiomes clinically isolated from young and young-adult patients. *J. Nanomater.* **2019**, *2019*, 3205971. [CrossRef]
58. Hall-Stoodley, L.; Costerton, J.W.; Stoodley, P. Bacterial biofilms: From the natural environment to infectious diseases. *Nat. Rev. Microbiol.* **2004**, *2*, 95–108. [CrossRef]
59. Al-Dhabi, N.A.; Ghilan AK, M.; Esmail, G.A.; Arasu, M.V.; Duraipandiyan, V.; Ponmurugan, K. Environmental friendly synthesis of silver nanomaterials from the promising *Streptomyces parvus* strain Al-Dhabi-91 recovered from the Saudi Arabian marine regions for antimicrobial and antioxidant properties. *J. Photochem. Photobiol. B Biol.* **2019**, *197*, 111529. [CrossRef]
60. Salem, S.S.; Fouda, A. Green synthesis of metallic nanoparticles and their prospective biotechnological applications: An overview. *Biol. Trace Elem. Res.* **2021**, *199*, 344–370. [CrossRef]
61. Al-Otibi, F.; Alfuzan, S.A.; Alharbi, R.I.; Al-Askar, A.A.; AL-Otaibi, R.M.; Al Subaie, H.F.; Moubayed, N.M. Comparative Study of Antifungal Activity of Two Preparations of Green Silver Nanoparticles from *Portulaca oleracea* Extract. *Saudi J. Biol. Sci.* **2022**, *29*, 2772–2781. [CrossRef]
62. Manivasagan, P.; Venkatesan, J.; Senthilkumar, K.; Sivakumar, K.; Kim, S.-K. Biosynthesis, antimicrobial and cytotoxic effect of silver nanoparticles using a novel *Nocardiopsis* sp. MBRC-1. *Biomed. Res. Int.* **2013**, *2013*, 287638. [CrossRef]
63. Singh, H.; Du, J.; Singh, P.; Yi, T.H. Ecofriendly synthesis of silver and gold nanoparticles by *Euphrasia officinalis* leaf extract and its biomedical applications. *Artif. Cells Nanomed. Biotechnol.* **2018**, *46*, 1163–1170. [CrossRef]
64. Navya, P.N.; Daima, H.K. Rational engineering of physicochemical properties of nanomaterials for biomedical applications with nanotoxicological perspectives. *Nano Converg.* **2016**, *3*, 1. [CrossRef] [PubMed]
65. Chithrani, B.D.; Chan, W.C. Elucidating the mechanism of cellular uptake and removal of protein-coated gold nanoparticles of different sizes and shapes. *Nano Lett.* **2007**, *7*, 1542–1550. [CrossRef] [PubMed]
66. Chithrani, B.D.; Ghazani, A.A.; Chan, W.C. Determining the size and shape dependence of gold nanoparticle uptake into mammalian cells. *Nano Lett.* **2006**, *6*, 662–668. [CrossRef]
67. Dacarro, G.; Pallavicini, P.; Bertani, S.M.; Chirico, G.; D'Alfonso, L.; Falqui, A.; Marchesi, N.; Pascale, A.; Sironi, L.; Taglietti, A.; et al. Synthesis of reduced-size gold nanostars and internalization in SH-SY5Y cells. *J. Colloid Interface Sci.* **2017**, *505*, 1055–1064. [CrossRef]
68. Thirunavoukkarasu, M.; Balaji, U.; Behera, S.; Panda, P.K.; Mishra, B.K. Biosynthesis of silver nanoparticle from leaf extract of *Desmodium gangeticum* (L.) DC. and its biomedical potential. *Spectrochim. Acta Part A Mol. Biomol. Spectrosc.* **2013**, *116*, 424–427. [CrossRef]
69. Seyedeh, M.G.; Sepideh, H.; Shojaosadati, S.A. Green synthesis of silver nanoparticles by a novel method: Comparative study of their properties. *Carbohydr. Polym.* **2012**, *89*, 467–472.
70. Kora, A.J.; Sashidhar, R.B.; Arunachalam, J. Aqueous extract of gumolibanum (*Boswellia serrata*): A reductant and stabilizer for the biosynthesis of antibacterial silver nanoparticles. *Process. Biochem.* **2012**, *47*, 1516–1520. [CrossRef]
71. Saranyaadevi, K.; Subha, V.; Ravindran, R.S.E.; Renganathan, S. Green synthesis and characterization of silver nanoparticle using leaf extract of *Capparis zeylanica*. *Asian J. Pharm. Clin. Res.* **2014**, *7*, 44–48.
72. Rai, M.K.; Deshmukh, S.D.; Ingle, A.P.; Gade, A.K. Silver nanoparticles: The powerful nanoweapon against multidrug-resistant bacteria. *J. Appl. Microbiol.* **2012**, *112*, 841–852. [CrossRef]
73. Verma, A.; Sanghi, S.; Grover, D.; Aggarwal, S.; Gupta, R.; Pandit, N. Effect of insertion of xanthan-based chlorhexidine gel in the maintenance phase following the treatment of chronic periodontitis. *J. Indian Soc. Periodontol.* **2012**, *16*, 381–385. [CrossRef] [PubMed]

74. Knight, E.T.; Liu, J.; Seymour, G.J.; Faggion, C.M., Jr.; Cullinan, M.P. Risk factors that may modify the innate and adaptive immune responses in periodontal diseases. *Periodontology* **2016**, *71*, 22–51. [CrossRef]
75. Ali, S.S.; Shaaban, M.T.; Abomohra, A.E.F.; El-Safity, K. Macroalgal activity against multiple drug resistant *Aeromonas hydrophila*: A novel treatment study towards enhancement of fish growth performance. *Microb. Pathog.* **2016**, *101*, 89–95. [CrossRef] [PubMed]
76. Freitas, R.D.; Dias, R.B.; Vidal, M.T.A.; Valverde, L.D.F.; Costa, R.G.A.; Damasceno, A.K.A.; Sales, C.B.S.; de Oliveira Siquara da Rocha, L.; Dos Reis, M.G.; Soares, M.B.P.; et al. Inhibition of CAL27 oral squamous carcinoma cell by targeting hedgehog pathway with vismodegib or itraconazole. *Front. Oncol.* **2020**, *2469*, 563838. [CrossRef] [PubMed]
77. Franci, G.; Falanga, A.; Galdiero, S.; Palomba, L.; Rai, M.; Morelli, G.; Galdiero, M. Silver nanoparticles as potential antibacterial agents. *Molecules* **2015**, *20*, 8856–8874. [CrossRef] [PubMed]
78. Khalil, M.A.E.F.; Sonbol, F.I.; Badr, A.; Ali, S.S. Comparative study of virulence factors among ESβL-producing and nonproducing *Pseudomonas aeruginosa* clinical isolates. *Turk. J. Med. Sci.* **2015**, *45*, 60–69. [CrossRef]
79. Khalil, M.A.; El-Sheekh, M.M.; El-Adawi, H.I.; El-Deeb, N.M.; Hussein, M.Z. Efficacy of microencapsulated lactic acid bacteria in *Helicobater pylori* eradication therapy. *J. Res. Med. Sci.* **2015**, *20*, 950. [CrossRef]
80. Khalil, M.; Ismail, M.M.; El Shafay, S.M. Evaluation of antibacterial activity of macroalgae extracts as adjunctive therapy in neonates sepsis induced by *Klebsiella pneumoniae*. *Arab. J. Sci. Eng.* **2020**, *45*, 4599–4607. [CrossRef]
81. Qing, Y.; Cheng, L.; Li, R.; Liu, G.; Zhang, Y.; Tang, X.; Wang, J.; Liu, H.; Qin, Y. Potential antibacterial mechanism of silver nanoparticles and the optimization of orthopedic implants by advanced modification technologies. *Int. J. Nanomed.* **2018**, *13*, 3311–3327. [CrossRef]
82. Abbaszadegan, A.; Ghahramani, Y.; Gholami, A.; Hemmateenejad, B.; Dorostkar, S.; Nabavizadeh, M.; Sharghi, H. The effect of charge at the surface of silver nanoparticles on antimicrobial activity against gram-positive and gram-negative bacteria: A preliminary study. *J. Nanomater.* **2015**, *16*, 53. [CrossRef]
83. Pandey, J.K.; Swarnkar, R.K.; Soumya, K.K.; Dwivedi, P.; Singh, M.K.; Sundaram, S.; Gopal, R. Silver nanoparticles synthesized by pulsed laser ablation: As a potent antibacterial agent for human enteropathogenic gram-positive and gram-negative bacterial strains. *Appl. Biochem. Biotechnol.* **2014**, *174*, 1021–1031. [CrossRef] [PubMed]
84. Deshmukh, S.P.; Patil, S.M.; Mullani, S.B.; Delekar, S.D. Silver nanoparticles as an effective disinfectant: A review. *Mater. Sci. Eng. C* **2019**, *97*, 954–965. [CrossRef] [PubMed]
85. Panáček, A.; Kvítek, L.; Prucek, R.; Kolář, M.; Večeřová, R.; Pizúrová, N.; Sharma, V.K.; Nevěčná, T.; Zbořil, R. Silver colloid nanoparticles: Synthesis, characterization, and their antibacterial activity. *J. Phys. Chem. B* **2006**, *110*, 16248–16253. [CrossRef] [PubMed]
86. Ghosh, S.; Patil, S.; Ahire, M.; Kitture, R.; Kale, S.; Pardesi, K.; Cameotra, S.S.; Bellare, J.; Dhavale, D.D.; Jabgunde, A.; et al. Synthesis of silver nanoparticles using *Dioscorea bulbifera* tuber extract and evaluation of its synergistic potential in combination with antimicrobial agents. *Int. J. Nanomed.* **2012**, *7*, 483.
87. Su, H.L.; Chou, C.C.; Hung, D.J.; Lin, S.H.; Pao, I.C.; Lin, J.H.; Huang, F.-L.; Dong, R.-X.; Lin, J.-J. The disruption of bacterial membrane integrity through ROS generation induced by nanohybrids of silver and clay. *Biomaterials* **2009**, *30*, 5979–5987. [CrossRef]
88. Quinteros, M.A.; Aristizábal, V.C.; Dalmasso, P.R.; Paraje, M.G.; Páez, P.L. Oxidative stress generation of silver nanoparticles in three bacterial genera and its relationship with the antimicrobial activity. *Toxicol. Vitr.* **2016**, *36*, 216–223. [CrossRef]
89. Morones, J.R.; Elechiguerra, J.L.; Camacho, A.; Holt, K.; Kouri, J.B.; Ramírez, J.T.; Yacaman, M.J. The bactericidal effect of silver nanoparticles. *Nanotechnology* **2005**, *16*, 2346. [CrossRef]
90. Manivasagan, P.; Venkatesan, J.; Sivakumar, K.; Kim, S.K. Actinobacteria mediated synthesis of nanoparticles and their biological properties: A review. *Crit. Rev. Microbiol.* **2016**, *42*, 209–221. [CrossRef]
91. Liao, C.; Li, Y.; Tjong, S.C. Bactericidal and cytotoxic properties of silver nanoparticles. *Int. J. Mol. Sci.* **2019**, *20*, 449. [CrossRef]
92. Chauhan, R.; Kumar, A.; Abraham, J. A biological approach to the synthesis of silver nanoparticles with Streptomyces sp. JAR1 and its antimicrobial activity. *Sci. Pharm.* **2013**, *81*, 607–624. [CrossRef]
93. Li, J.; Rong, K.; Zhao, H.; Li, F.; Lu, Z.; Chen, R. Highly selective antibacterial activities of silver nanoparticles against Bacillus subtilis. *J. Nanosci. Nanotechnol.* **2013**, *13*, 6806–6813. [CrossRef] [PubMed]
94. Jung, W.K.; Koo, H.C.; Kim, K.W.; Shin, S.; Kim, S.H.; Park, Y.H. Antibacterial activity and mechanism of action of the silver ion in *Staphylococcus aureus* and *Escherichia coli*. *Appl. Environ. Microbiol.* **2008**, *74*, 2171–2178. [CrossRef] [PubMed]
95. Mhaske, A.R.; Shetty, P.C.; Bhat, N.S.; Ramachandra, C.S.; Laxmikanth, S.M.; Nagarahalli, K.; Tekale, P.D. Antiadherent and antibacterial properties of stainless steel and NiTi orthodontic wires coated with silver against Lactobacillus acidophilus—An in vitro study. *Prog. Orthod.* **2015**, *16*, 40. [CrossRef] [PubMed]
96. Zaki, A.; Aziz, M.N.; Ahmad, R.; Ahamad, I.; Ali, M.S.; Yasin, D.; Afzal, B.; Ali, S.M.; Chopra, A.; Hadda, V.; et al. Synthesis, purification and characterization of Plectonema derived AgNPs with elucidation of the role of protein in nanoparticle stabilization. *RSC Adv.* **2022**, *12*, 2497–2510. [CrossRef] [PubMed]

97. Jiménez-Ramírez, A.J.; Martínez-Martínez, R.E.; Ayala-Herrera, J.L.; Zaragoza-Contreras, E.A.; Domínguez-Pérez, R.A.; Reyes-López, S.Y.; Donohue-Cornejo, A.; Cuevas-González, J.C.; Silva-Benítez, E.L.; Espinosa-Cristóbal, L.F. Antimicrobial activity of silver nanoparticles against clinical biofilms from patients with and without dental Caries. *J. Nanomater.* **2021**, *2021*, 5587455. [CrossRef]
98. Charulatha, V.; Rajaram, A. Influence of different crosslinking treatments on the physical properties of collagen membranes. *Biomaterials* **2003**, *24*, 759–767. [CrossRef]